In situ scanning tunneling microscopic and spectroscopic investigation of magnetron-sputtered C and CN thin films

Nian Lin*
Thin Film Physics Division, Department of Physics, Linköping University, S-581 83 Linköping, Sweden
Applied Physics Division, Department of Physics, Linköping University, S-581 83 Linköping, Sweden

Niklas Hellgren, Mats P. Johansson, and Lars Hultman
Thin Film Physics Division, Department of Physics, Linköping University, S-581 83 Linköping, Sweden

Ragnar Erlandsson
Applied Physics Division, Department of Physics, Linköping University, S-581 Linköping, Sweden

Jan-Eric Sundgren
Thin Film Physics Division, Department of Physics, Linköping University, S-581 83 Linköping, Sweden
and Office of the President, Chalmers University of Technology, S-412 96 Göteborg, Sweden
(Received 23 June 1999)

Carbon and carbon nitride films, grown in argon or nitrogen discharges by reactive dc magnetron sputtering of a graphite target, were characterized by *in situ* scanning tunneling microscopy. When the growth temperature increased from ambient to 800 °C, we observed a topographic evolution of the carbon films from an amorphous to a graphitelike structure, and further to a distorted-graphitic phase with curved and intersecting basal planes, and finally to a surface containing nanotubes and nanodomes. When nitrogen was incorporated into the films, distortion of the graphitic basal planes occurred at a lower temperature compared to the pure carbon case. At temperatures of ~200 °C and above, regions of a nongraphitic phase, containing a high degree of carbon sp^3 bonds were observed. Spatially resolved tunneling spectroscopic measurements indicated that the band gaps were 0, ~0-0.6 eV, and ~0.4-2.0 eV for graphitelike structures, the distorted-graphitic phase, and the nongraphitic phase, respectively. Together with *ex situ* x-ray photoelectron spectroscopy and reflection electron energy loss spectroscopy measurements, the results suggest that the incorporation of nitrogen promotes bending of the graphitic basal planes and thereby facilitates the formation of three-dimensional covalently bonded networks with a high degree of sp^3-coordinated carbon atoms.

I. INTRODUCTION

Carbon-based hard materials, such as diamondlike carbon and carbon nitride (CN_x) thin films, have gained extensive attention because of their wide spread technological applications, e.g., as tribological and wear resisting coatings.[1] The structure, chemistry, and morphology of such films have been characterized, among other techniques, by transmission electron microscopy (TEM), electron energy loss spectroscopy (EELS), and scanning electron microscopy (SEM). TEM in combination with EELS have shown to be a particularly useful tool, since it combines high-resolution imaging with the possibility to obtain local chemical information.[2]

Physical vapor-deposited diamondlike carbon films, having a high degree of sp^3 bonds, are normally found to be amorphous. However, graphitic or turbostratic carbon films can also be found, especially when deposited at elevated temperatures. Carbon nitride films are also normally amorphous for low-growth temperatures, but evolves into a more ordered turbostraticlike structure at temperatures above ~200 °C.[3] This phase has been found to be hard, but also highly elastic, a property that has been ascribed to a microstructure consisting of frequently cross-linked and curved graphitic basal planes.[4] It was proposed that the basal planes curve due to the incorporation of pentagons, which is facilitated by the substitution of nitrogen. Curved basal planes would, in turn, promote cross linking between two neighboring planes through sp^3 bonds. By virtue of such basal plane curvature and the possible presence of pentagons, the structure has been defined as ''fullerenelike.''[4] Several experimental results support this interpretation,[5] however, it is difficult to unambiguously confirm the presence of cross links, e.g., by TEM, EELS, or x-ray photoelectron spectroscopy (XPS).

Using scanning tunneling microscopy (STM), the surface structure of such compounds can be studied with atomic resolution. However, due to surface reconstructions and contaminations occurring when the film is exposed to the atmosphere, *ex situ* analysis does not give information about the atomic structure during growth. Therefore, in order to gain an increased understanding about the structural evolution during growth of such films, *in situ* characterization is necessary.

In this paper, we present atomic-scale topographic and electronic analysis of *in situ* prepared carbon and carbon nitride films. Films were deposited by magnetron sputtering at various temperatures between ambient and 800 °C, in order to study the structural evolution under various growth con-

ditions. The films were then studied *ex situ* by XPS and reflection electron energy loss spectroscopy.

II. EXPERIMENTAL DETAILS

Carbon and carbon nitride films were deposited onto clean Si(001) substrates by unbalanced dc magnetron sputtering in a preparation chamber having a background pressure of $\sim 3\times 10^{-10}$ Torr. The target was a high-purity 99.99% pyrolytic graphite disc, 30 mm in diameter, mounted on a planar magnetron cathode. The depositions were carried out at a pressure of 10 mTorr, either in Ar of 99.9999% purity level, or 99.999% pure N_2. The discharge was operated at a constant power of 20 W and with a current between 36 and 42 mA. The substrates, which were mounted 100 mm from the target, were held at a negative floating potential of $\sim$30 to 40 V. With a plasma potential of $\sim$10–20 V, as measured by a Langmuir probe, this corresponds to an incident N_2^+ energy of $\sim$20 eV. The Si(001) samples were cleaned by the standard RCA method[6] before being introduced into the growth chamber, and were then flashed to 1150 °C in the vacuum in order to remove residual oxides. The substrates were then clean and flat as observed by *in situ* STM before deposition, and the atomically resolved dimer rows on the Si(001) surfaces could be routinely imaged. The target was sputter cleaned for 3 min before each deposition, with the substrates facing away from the target. The substrates were heated to the desired temperature by passing a current through the silicon. The temperatures above 550 °C were accurately monitored by an infared (IR) pyrometer, while temperatures below 550 °C were determined by the power of the passing current. The power vs temperature calibration had been performed previously by a thermocouple. A series of depositions were made at different substrate temperatures, ranging from room temperature to 800 °C. The deposited films were then transferred *in vacui* into the analysis chamber equipped with a home-built UHV STM.[7] The background pressure of the STM chamber was kept below 1×10^{-10} Torr. All the images shown in the paper were taken from films thicker than 20 nm, and processed by the statistical differentiating method[8] in order to improve the visibility of small structural features. This image processing enhances the contrast on flat areas, and reduces the sensitivity on areas with large height variations. Thus atomic corrugation becomes visible on different surface layers, in spite of the height differences. No artifacts are introduced, besides that the true three-dimensional picture may become somewhat distorted. After the *in situ* measurements, the films were analyzed *ex situ* by XPS and REELS (see Ref. 5 for experimental details). The growth rate was also determined afterwards using a surface profilometer.

III. RESULTS AND DISCUSSION

3.1. Carbon films

The results showed that independent of the growth conditions, the first several monolayers of the films were amorphous or disordered. However, after a few nm thickness a microstructure evolved, which was then maintained during growth. When increasing the growth temperature, a gradual transition in surface topography could be observed for both carbon and carbon nitride films. Figure 1 shows typical surface topography of the pure carbon films deposited at room temperature (a), 350 °C (b) and 800 °C (c), respectively. The close view images (to the right) show the detailed features of the square box areas. The surface of the room temperature-deposited films was amorphous as we could not identify any order. When the growth temperature was increased above 200 °C, regions consisting of parallel ''stripes'' appeared on the otherwise amorphous films, as can be seen in Fig. 1(b) for a film deposited at 350 °C. The distance between neighboring ''stripes'' was 0.35 ± 0.02 nm, which agrees well with the interplanar distance of graphite basal planes (0.335 nm). We believe that the ''stripes'' are the cross-sectional view of the graphite basal planes, consistent with previous reports,[3,9] which have shown that carbon films grown at these conditions have a graphitelike structure with the *c* axis preferentially oriented in the plane of the film surface (vertical basal planes). The area fraction of amorphous regions decreased with increasing deposition temperature. However, even at the highest growth temperature of our experiments, there still

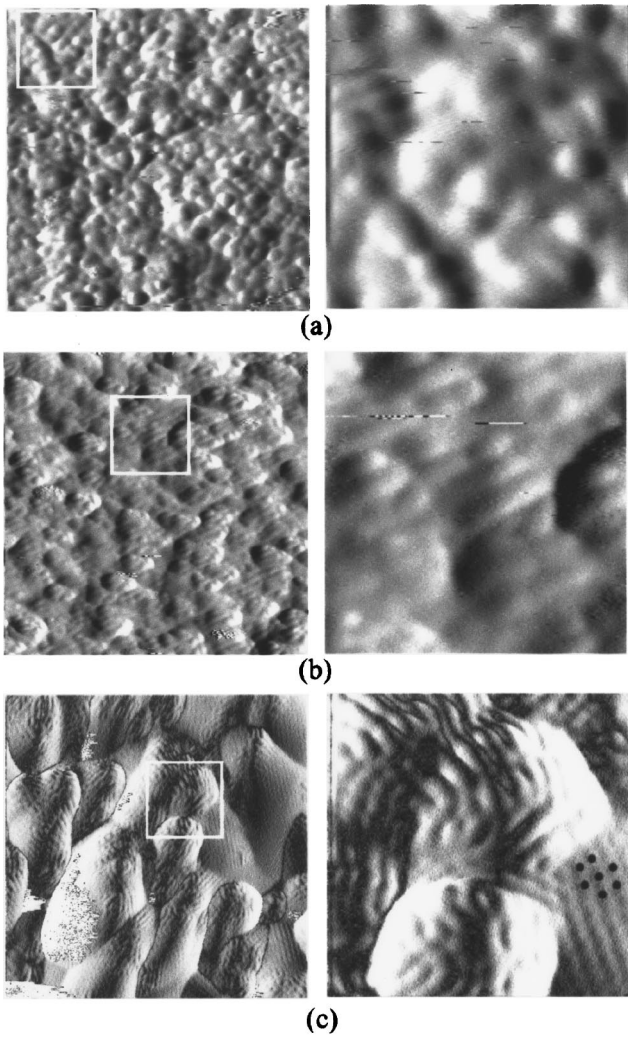

FIG. 1. STM images of surface topography of the pure carbon films grown at (a) room temperature, (b) 350 °C, and (c) 800 °C. Right images are close views of the square box areas of the left images. The size of the left images is 18 nm×18 nm and the enlarged images are 4.5 nm×4.5 nm. Images have been processed by the statistical differentiating method. (Ref. 8)

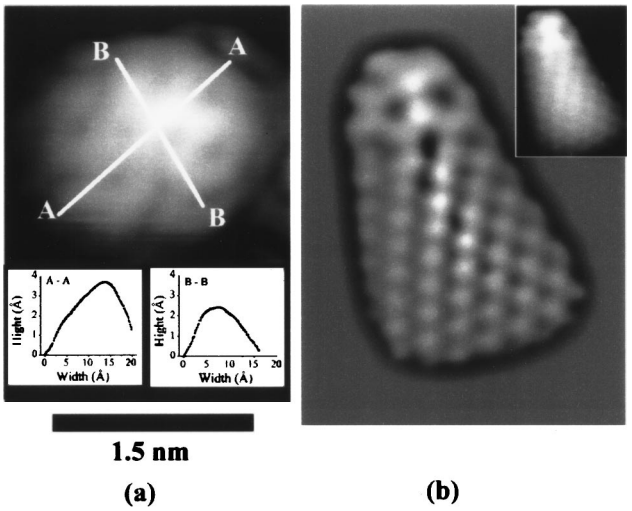

FIG. 2. STM images of (a) a nanodome structure and (b) a conical nanotube with a $26.5 \pm 1.0°$ cone angle, found on a film grown at 800 °C. The same scale is used in both images. The inset images in (a) show two line profiles revealing the curvature of the dome. Image (b) has been processed by the statistical differentiating method and the small inset shows the raw image.

existed small regions of amorphous or disordered surface. When the growth temperature was increased above 500 °C, the ''stripes'' were, in most cases, curved in a wavelike fashion, indicating that the graphite basal planes were distorted at these temperatures. The distortion of the basal planes was even more pronounced for the films grown at 800 °C, as illustrated in Fig. 1(c). Some basal planes were also found to be curved such that their *c* axes were almost normal to the film plane (horizontal basal planes), as can be seen in the lower-right corner of the square box area. Here, a hexagonal structure is revealed, highlighted by the solid dots, with a nearest-neighbor distance of 0.25 ± 0.02 nm, comparable to that of graphite seen by STM (0.246 nm).

At the higher temperatures (above 500 °C) we also observed other types of interesting structures, such as nanometer-scale domes, and tubular nanostructures, as illustrated in Fig. 2. An example of the domes is given in Fig. 2(a). Two line profiles (inset images) over the surface of the nanodome reveal spherical shape of the dome. The dome is build up from connected aromatic rings, and the diameter of the rings was 0.30 ± 0.02 nm, similar to the size of the pentagonal or hexagonal rings of a C_{60} molecule. The image can not reveal whether it is a pentagon or a hexagon, but odd-membered rings must be involved to form spherical structures. The half dome thus might be part of a fullerene-type molecule or an end cap of a nanutube. Figure 2(b) shows an example of a nanotubelike feature with a $26.5 \pm 1.0°$ cone angle, and with a half-dome cap at its end.

The high lateral resolution of the STM makes it an ideal tool for studying how the local electronic properties vary spatially on a nanometer-scale.[10,11] While ramping the bias voltage between the tip and the sample, when separated by a constant distance, the recorded tunneling current is a representation of the local density of states (DOS) of the sample surface. Here, we employed tunneling spectroscopy to study the electronic properties of the specific nanometer-scale structures observed in the films. It was found that both carbon and carbon nitride films had very high resistivity if the film thickness was less than ~2 nm, and no tunneling current was recorded for bias voltages between +5 and −5 V. The resistivity dropped rapidly when increasing the film thickness and stayed constant for films thicker than 10 nm. The resistivity of thick films as measured by a four-point probe was $\sim 4 \times 10^{-3}\ \Omega$-cm.[12] The high resistivity of very thin films can be explained by the probable formation of an insulating SiC or $Si_xC_{1-x}N$ interface layer between the films and the Si substrates, which would act as a barrier preventing the tunneling current running away. For the thicker films, tunneling current could be transported in the films because of their good conductivity, and be conducted away through the metal sample holder, which contacted the edges of the films. The contribution of the Si substrates to the tunneling characteristics between the tip and the film can thus be expected to be negligible.

The good conductivity of the thicker films allowed us to view the specific nanometer-scale structures with nonzero band gaps as islands in a conducting sea. Because of the charge transfer to and from the surroundings, the band structure of a specified structure obtained from its tunneling spectra would not equal the DOS of the isolated nanometer-scale structure. However, the tunneling spectra would still provide information about the local electronic properties. The tunneling spectroscopic measurements were repeated 20 to 30 times at each measuring point and showed very good reproducibility. Images were taken before and after the tunneling spectroscopic measurements as references to guarantee the spatial accuracy of the tunneling spectroscopy. For the pure carbon films, we measured the tunneling spectra of various types of representative structures: the amorphous phase, graphitelike phases with standing and lying basal planes, respectively, the distorted-graphitic phase with wavelike basal planes, as well as the nanodome features. The overall characters of the current vs voltage (I-V) curves repeated very well for the same kinds of structures. In Fig. 3, I-V curves are plotted, as well as dI/dV vs V and $(V/I)(dI/dV)$ vs V curves since they are good approximations to the local DOS.[13] The graphitelike phase had a metallic behavior, as shown in Fig. 3(a), whose DOS is nonzero near the zero-bias voltage, i.e., the Fermi level. The band structures of the distorted basal planes, both vertical ones and horizontal ones, displayed transitional features. Some of them have a gapless behavior, [as Fig. 3(b) shows], but the apparent low conductance near the zero bias means that the DOS is very small around the Fermi level, as indicated by the dI/dV curve. In some cases, the conductance near the zero bias reduced to zero so that there appeared a gap of zero DOS, as shown in Fig. 3(c). Figure 3(d) shows a typical tunneling spectrum of a nanodome, indicating a band gap of ~0.3 eV. The width of the band gaps varied from 0.2 to 0.6 eV for different nanodomes. The reason why these curved graphitic planes have such a broad distribution of band gaps is not clear. It is well known that a perfect sp^2-bonded graphite has a zero band gap, while the sp^3-bonded diamond structure has a band gap as large as 5.5 eV. However, since the band gaps recorded here were in most cases $\leqslant 0.6$ eV, we conclude that these films were predominantly sp^2 coordinated. This was also confirmed by the *ex situ* REELS measurements, which showed a significant signal from $\pi(sp^2)$ bonds for the car-

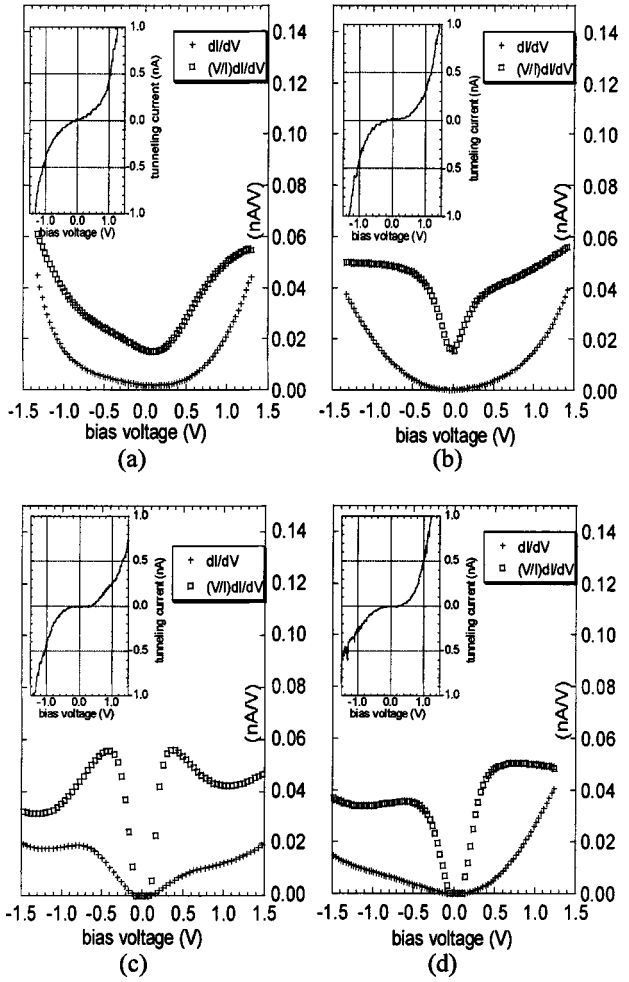

FIG. 3. Local tunneling spectra I-V (inset), dI/dV-V (cross), and $(V/I)(dI/dV)$-V (square) measured on the different structures of the pure carbon films. (a) The graphitelike phase; (b) and (c), the distorted-graphitic phase; (d) the nanodomes. The bias voltage was applied to the tip, which means that the positive bias corresponds to the filled states and negative bias to the empty states.

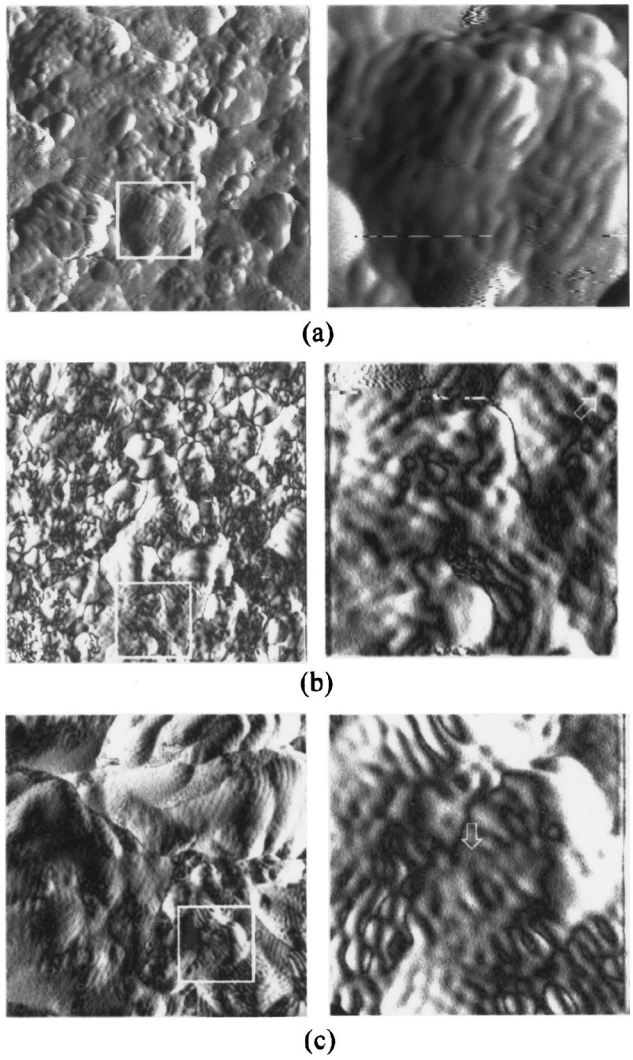

FIG. 4. STM images of surface topography of the carbon nitride films grown at 350 °C (a) and (b), 500 °C (c). Right images are close views of the square box areas of the left images. The size of the left images is 18 nm×18 nm and the enlarged images are 4.5 nm×4.5 nm. Images have been processed by the statistical differentiating method. (Ref. 8)

bon films grown above 300 °C. The local variations of the band gap could be the result of the distortion of the graphite planes, meaning not only incorporation of sp^3 bonds, but also curvature and the presence of odd-membered rings. A recent report has suggested that the electronic structures of nanotubes would be sensitive to the position of pentagons and their degree of confinement at the tube ends.[14] Highly curved nanodomes and distorted graphite planes, such as those observed here, are likely to involve more pentagons, which would result in more band structure distortion.

Furthermore, tunneling spectra of the amorphous films, grown at low temperature, were measured, showing band gaps ranging from 0 up to 2.0 eV. Because of the amorphous nature of the film, the tunneling spectra could not be correlated to any specific geometric structures. Considering the 0.6-eV band gap upper limit of the predominantly sp^2-coordinated films grown at higher temperatures discussed above, it is not likely that these large band gaps were solely caused by distortion of the sp^2 bonds. However, a somewhat larger fraction of sp^3-coordinated carbon, which can be expected in the amorphous carbon films, could probably explain the increased band gap.[15] Nevertheless, both theoretical and experimental efforts are required to unravel the electronic properties of sp^2/sp^3 hybrid system.

3.2. Carbon nitride films

Carbon nitride films were grown at different temperatures and studied by *in situ* STM. The room temperature-grown CN_x films had the highest nitrogen concentration as determined by XPS (~30 at. %). For increasing growth temperatures, the nitrogen concentration reduced gradually, and was found to be ~15 at. % at 600 °C. This trend is consistent with previously reported results.[16] Similar to the pure carbon films, CN_x films grown below 200 °C exhibited an amorphous structure. When increasing the temperature up to 350 °C, however, a distorted-graphitic phase of curved basal planes gradually emerged out of the amorphous/disordered background, as shown in Fig. 4(a). While the distortion of graphite planes for pure carbon films took place above

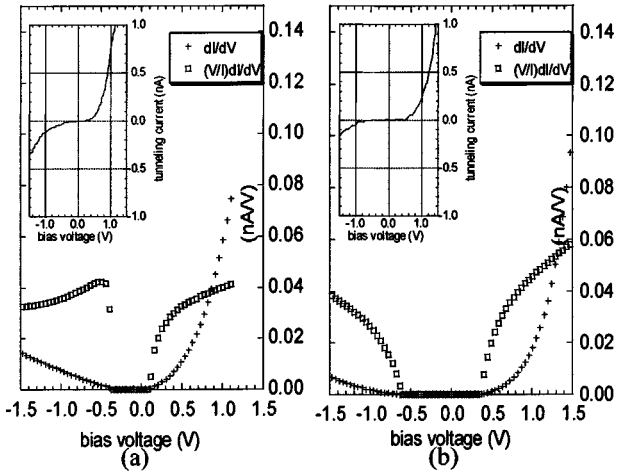

FIG. 5. Local-tunneling spectra I-V (inset), dI/dV-V (cross), and $(V/I)(dI/dV)$-V (square) of the CN_x films. (a) Distorted-graphitic phase and (b) nongraphitic phase. The bias voltage was applied to the tip, which means that the positive bias corresponds to the filled states and negative bias to the empty states.

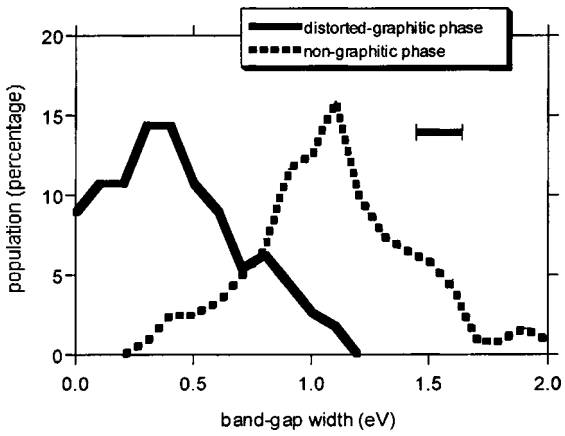

FIG. 6. Statistical distribution of the band gap width of the distorted-graphitic phase (solid line) and the nongraphitic phase (dashed line) measured on the same CN_x film grown at 500 °C. Experimental error of the band-gap width was 0.2 eV, as indicated by the error bar.

500 °C, it occurred at ~350 °C for the CN_x films. This difference is likely caused by nitrogen substitution in the graphite sites. This observation would support previous quantum chemical calculations indicating that the nitrogen atoms prefer a nonplanar surrounding.[4,17] Apart from the distorted-graphitic phase, we also observed regions on the 350 °C grown CN_x films consisting of graphitic planes that appears to be cross linked and intersected, as shown in Fig. 4(b). The enlarged view indicates that the neighboring ''stripes'' were frequently linked together by interplanar bridges (pointed by the arrow), resulting in three-dimensional networks. These regions were different from the graphitic phases. It illustrates a 0.20 ± 0.02-nm spaced network with a nearly 90° bond angle. This inter planar distance is comparable, e.g., to the (111) plane distance of diamond (0.206 nm). However, the cubic symmetry, and the fact that high-resolution TEM have not revealed any crystalline regions in CN_x films grown by magnetron sputtering at elevated temperatures,[3] indicate that these regions do not correspond to diamond, or any other crystalline structure. Instead, we believe that the short plane distance may be due to distorted graphite planes, which are forced together due to sp^3-bonded carbon cross links. The detailed bonding structure is, however, unclear and we define this type of structures as nongraphitic phase.

When further increasing the growth temperature, more disordered/amorphous regions transformed into the distorted graphitic, both with vertical and horizontally oriented basal planes, but somewhat less regions with the non-graphitic phase could be seen. Figure 4(c) is an image of the surface of a 500 °C grown CN_x film, which exhibits an appearance similar to that of the pure carbon films grown at the same temperature, however, more regions where the basal planes merged together, or were possibly cross-linked could be observed. The arrow in the enlarged image marks a point where different basal planes seem to merge. This further supports the observation that the nitrogen incorporation distorts the graphitic structure.

The tunneling spectra of the distorted-graphitic phase of the CN_x films resembled those of the pure carbon films, with a band gap typically below 0.6 eV, as displayed in Fig. 5(a). The non-graphitic phase, however, had a much wider band gap of ~0.4-2.0 eV, as shown in Fig. 5(b). Figure 6 displays statistical distributions of the band gap width for the distorted-graphitic phase and the non-graphitic phase measured on the same CN_x film. Totally 80 tunneling spectra were recorded from different areas of the two structures. The graph presents the counts of spectra having a specific band gap, where the number of the spectra whose band gap width are in the interval $E-0.05$ eV to $E+0.05$ eV is represented by the population at energy E, where E is 0.00 eV, 0.10 eV, 0.20 eV, ..., 2.00 eV. It can be seen that the band gaps of the two different types of structures falls into two categories. The band gaps of the distorted-graphitic phase center at ~0.4 eV, while the non-graphitic phase center at ~1.1 eV. We believe that the wide band gap present here originates from a higher local density of sp^3-coordinate carbon atoms. We also detected ~2.0 eV band gaps on the amorphous pure carbon films that are known to have a higher sp^3 fraction. Therefore, it is reasonable to ascribe the large band gaps of the nongraphitic phase to a high local density of sp^3-coordinated carbon structure. Regions with a locally lower sp^3-concentration appear as a distorted-graphitic structure, which coexists with the nongraphitic structures.

The present results support previous indications[5] that incorporation of nitrogen into the graphitic carbon structure leads to a distortion of the basal planes and thereby facilitate cross links between the planes as they come closer together. Similar kinds of distortions were also observed in the pure carbon films, but at higher temperatures. The spectroscopic measurements further suggested that regions of high fraction of sp^3 bonds were formed in the nitrogen containing samples. However, since the overall conductivity of all films was very good, we conclude that the structures were predominantly graphitic, but due to the distortion of the basal planes, cross links between the planes, and other regions, could have a high local fraction of sp^3-coordinated carbon.

IV. CONCLUSIONS

In conclusion, the carbon films grown at temperatures above 300 °C by dc magnetron sputtering were highly

graphitelike, in other words, they were quite well ordered and were dominated by the $\pi(sp^2)$ bonding. The bond angles became deformed at elevated growth temperatures. Consequently, the graphite basal planes were distorted. The deformation of the geometric structures also changed their electronic properties, and the local tunneling spectra revealed that those distorted-graphitic structures have a broad spread of band gaps from zero to 0.6 eV. In the presence of nitrogen, the basal plane distortion occurred at lower temperatures compared to the pure carbon films and, a nongraphitic phase having larger band gaps developed, indicating a higher density of sp^3-coordinated carbon. Thus, the incorporation of nitrogen promotes curving of the basal planes, and regions with a high degree of sp^3 bonds were formed, presumably where the graphitic structure was the most distorted.

ACKNOWLEDGEMENTS

The financial support from the Material Research Consortium on Thin Film Growth, through the Swedish Foundation for Strategic Research (SSF), is greatly appreciated.

*Author to whom correspondence should be addressed. Electronic address: niali@ifm.liu.se. Present address: Max-Planck-Institute FKF, Heisenbergstrasse 1, 70569 Stuttgart, Germany.

[1] See, e.g., A. Grill, Surf. Coat. Technol. **94-95**, 507 (1997), and references therein.

[2] K. Suenaga, M. P. Johansson, N. Hellgren, E. Broitman, L. R. Wallenberg, C. Colliex, J.-E. Sundgren, and L. Hultman, Chem. Phys. Lett. **300**, 695 (1999).

[3] H. Sjöström, L. Hultman, J.-E. Sundgren, S. V. Hainsworth, T. F. Page, and G. S. A. M. Theunissen, J. Vac. Sci. Technol. A **14**, 56 (1996).

[4] H. Sjöström, S. Stafström, M. Boman, and J.-E. Sundgren, Phys. Rev. Lett. **75**, 1336 (1995).

[5] N. Hellgren, M. P. Johansson, E. Broitman, L. Hultman, and J.-E. Sundgren, Phys. Rev. B **59**, 5162 (1999).

[6] W. Kern and D. A. Puotinen, RCA Rev. **31**, 187 (1970).

[7] F. Owman, Ph.D. Thesis No. 420, Linköping University, Linköping, 1996.

[8] W. K. Pratt, *Digital Image Processing* (Wiley, New York, 1978).

[9] N. Hellgren, M. P. Johansson, E. Broitman, P. Sandström, L. Hultman, and J.-E. Sundgren (unpublished).

[10] J. W. G. Wildoer, L. C. Venema, A. G. Rinzler, R. E. Smalley, and C. Dekker, Nature (London) **391**, 59 (1998).

[11] T. W. Odom, J-L. Huang, P. Kim, and C. M. Lieber, Nature (London) **391**, 62 (1998).

[12] E. Broitman, N. Hellgren, K. Järrendahl, M. P. Johansson, S. Olafsson, J.-E. Sundgren, and L. Hultman (unpublished).

[13] J. A. Stroscio and R. M. Feenstra, in *Scanning Tunneling Microscopy*, edited by J. A. Stroscio and R. M. Feenstra (Academic, New York, 1993), pp. 95–141.

[14] D. L. Carroll, P. Redlich, P. M. Ajayan, J. C. Charlier, X. Blasé, A. De Vita, and R. Car, Phys. Rev. Lett. **78**, 2811 (1997).

[15] J. J. Cuomo, D. L. Pappas, J. Bruley, J. P. Doyle, and K. L. Saenger, J. Appl. Phys. **70**, 1706 (1991).

[16] H. Sjöström, I. Ivanov, M. Johansson, L. Hultman, J.-E. Sundgren, S. V. Hainsworth, T. F. Page, and L. R. Wallenberg, Thin Solid Films **246**, 103 (1994).

[17] M. C. dos Santos and F. Alvarez, Phys. Rev. B **58**, 13 918 (1998).